© 2023. Published by The Company of Biologists Ltd | Journal of Experimental Biology (2023) 226, jeb244721. doi:10.1242/jeb.244721

RESEARCH ARTICLE

Understanding muscle function during perturbed *in vivo* locomotion using a muscle avatar approach

Nicole Rice[1], Caitlin M. Bemis[1], Monica A. Daley[2] and Kiisa Nishikawa[1,*]

ABSTRACT

The work loop technique has provided key insights into *in vivo* muscle work and power during steady locomotion. However, for many animals and muscles, *ex vivo* experiments are not feasible. In addition, purely sinusoidal strain trajectories lack variations in strain rate that result from variable loading during locomotion. Therefore, it is useful to develop an 'avatar' approach in which *in vivo* strain and activation patterns from one muscle are replicated in *ex vivo* experiments on a readily available muscle from an established animal model. In the present study, we used mouse extensor digitorum longus (EDL) muscles in *ex vivo* experiments to investigate *in vivo* mechanics of the guinea fowl lateral gastrocnemius (LG) muscle during unsteady running on a treadmill with obstacle perturbations. *In vivo* strain trajectories from strides down from obstacle to treadmill, up from treadmill to obstacle, strides with no obstacle and sinusoidal strain trajectories at the same amplitude and frequency were used as inputs in work loop experiments. As expected, EDL forces produced with *in vivo* strain trajectories were more similar to *in vivo* LG forces (R^2=0.58–0.94) than were forces produced with the sinusoidal trajectory (average R^2=0.045). Given the same stimulation, *in vivo* strain trajectories produced work loops that showed a shift in function from more positive work during strides up from treadmill to obstacle to less positive work in strides down from obstacle to treadmill. Stimulation, strain trajectory and their interaction had significant effects on all work loop variables, with the interaction having the largest effect on peak force and work per cycle. These results support the theory that muscle is an active material whose viscoelastic properties are tuned by activation, and which produces forces in response to deformations of length associated with time-varying loads.

KEY WORDS: Guinea fowl, Muscle mechanics, Muscle fascicle strain, Viscoelastic properties, Work loop

INTRODUCTION

Decades of research on isolated muscles, single fibers and motor proteins has led to a widely accepted understanding of muscle mechanics based on the sliding filament–swinging cross-bridge theory (Huxley and Hanson, 1954; Huxley and Niedergerke, 1954; Rayment et al., 1993). Early studies emphasized the isometric force–length relationship (Gordon et al., 1966) and the isotonic force–velocity relationship (Hill, 1938), which was shown to be consistent with cross-bridge models of muscle contraction (Huxley, 1957, 1973). Compared with these traditional *ex vivo* methods for investigating muscle mechanics (i.e. isometric force–length and isotonic force–velocity relationships; Caiozzo, 2002), the work loop technique (Josephson, 1985) revolutionized the study of *ex vivo* muscle function (Ahn, 2012) by stimulating muscles during sinusoidal length oscillations at a frequency, phase and duty cycle similar to conditions that muscles experience during *in vivo* locomotion (Josephson, 1985, 1999). These studies enabled estimation of the work and power that muscles produce under *in vivo* conditions, compared with their maximum work and power output (Askew and Marsh, 1997; Askew et al., 1997; Full et al., 1998; Sponberg and Full, 2008; Sponberg et al., 2011; Tytell et al., 2018).

Work loop experiments also led to the insight that muscle function depends on the phase of activation relative to oscillations in length (Dickinson et al., 2000; Ahn et al., 2003). Muscles function like motors that perform positive work when stimulated at the onset of shortening, but like brakes that absorb work when stimulated during lengthening (Hessel and Nishikawa, 2017), or as struts and springs, producing little net work when stimulated during intermediate phases of the strain cycle (Ahn et al., 2003). These studies suggested that the role a muscle performs is determined largely by the timing of neural activation (Ahn et al., 2003; Ahn, 2012; Sponberg and Daniel, 2012).

Because of the technical difficulty of the measurements, relatively few studies have investigated muscle mechanics *in vivo*. *In vivo* animal studies have used sonomicrometry crystals to measure fascicle strain, electromyography (EMG) to measure activation, and tendon buckles to measure muscle force (Biewener et al., 1998; Daley et al., 2009; Daley and Biewener, 2011; Eng et al., 2019; Lee et al., 2013; Gordon et al., 2020; Roberts et al., 1997; Wakeling et al., 2021). These measurements are more difficult to make in humans, so muscle forces are typically estimated using inverse dynamics (Sylvester et al., 2021) rather than measured directly. However, a few recent studies have used ultrasound in humans (Dick et al., 2017) to measure not only muscle strain but also tendon strain, which should be proportional to muscle force.

Hill-type muscle models based on force–length and force–velocity relationships (Zajac, 1989; Seth et al., 2011) have been used to predict *ex vivo* (Stevens, 1993; James et al., 1995, 1996; Askew and Marsh, 1997; Perreault et al., 2003) and *in vivo* muscle forces (Lee et al., 2013; Dick et al., 2017; Wakeling et al., 2021). Yet, the results of these studies show that the force predictions of Hill-type models are relatively inaccurate (R^2<0.6), especially at higher frequencies (James et al., 1996; Wakeling et al., 2021). The inability of Hill-type models based on the isometric force–length and isotonic force–velocity relationships to accurately predict muscle force in *ex vivo* experiments and during *in vivo* locomotion suggests that our understanding of muscle mechanics is incomplete (Umberger and Rubenson, 2011), and that some concept(s) or element(s) may be missing from the model.

[1]Department of Biological Sciences, Northern Arizona University, Flagstaff, AZ 86011, USA. [2]Department of Ecology and Evolutionary Biology, University of California, Irvine, Irvine, CA 92697, USA.

*Author for correspondence (Kiisa.Nishikawa@nau.edu)

M.A.D., 0000-0001-8584-2052; K.N., 0000-0001-8252-0285

Received 29 June 2022; Accepted 8 June 2023

Journal of Experimental Biology (2023) 226, jeb244721. doi:10.1242/jeb.244721

One major limitation of both sinusoidal work loops and the force–velocity relationship is that they fail to include variability in muscle strain and loading rates that is typically observed during *in vivo* locomotion (Daley and Biewener, 2011). No current theory predicts muscle force during active shortening under time-varying loads and this is an important knowledge gap in muscle mechanics (Sponberg et al., 2023). Several new methods have been developed recently to overcome this limitation. For example, a novel bio-robotics approach has been used to apply realistic hydrodynamic loads to muscles using real-time feedback control, leaving the strain trajectory as the unconstrained and measured output variable (Richards, 2011; Richards and Clemente, 2012; Clemente and Richards, 2012; Robertson and Sawicki, 2015; Robertson et al., 2017). A similar approach was used by Olberding et al. (2019), who developed a computer model of limb extension during jumping to provide more realistic time-varying loads in *ex vivo* work loop experiments. However, these approaches are limited to relatively simple variations in loading that are amenable to either experimental manipulation or computational modeling. It remains to be discovered how naturally occurring variability in strain rates affects muscle force and work.

Technical advances have made it possible to measure *in vivo* strain and activation of individual muscles across a wide range of species and movement conditions, although direct measurements of force remain challenging for some muscles and species. To improve our understanding of variability in muscle function during *in vivo* conditions including perturbed locomotion, we developed a new method to bridge the gap between traditional *ex vivo* sinusoidal work loop experiments and *in vivo* locomotion. This method uses a well characterized muscle (extensor digitorum longus, EDL) from a laboratory rodent (mouse) as an 'avatar' to represent muscles that are difficult or impossible to study in *ex vivo* experiments. The method is otherwise similar to previous approaches using *ex vivo* work loop experiments to emulate *in vivo* strain and activation (e.g. Askew and Marsh, 1998, 2001; Sponberg et al., 2011). Development and validation of this avatar method enables testing the role that dynamic changes in strain and loading play during *in vivo* movements across a wide range of animals and muscles. We chose the term 'avatar' to describe use of the mouse EDL muscle to represent a different muscle in the *ex vivo* experimental environment, in which length and activation can be precisely controlled and the resulting forces measured.

The goal of the present study was to develop and validate the avatar method, and use it to investigate the contributions of naturally occurring small variations in muscle length and activation patterns to force production, measured in guinea fowl during a single trial of treadmill running with obstacle perturbations (Daley and Biewener, 2011). These obstacle perturbations produced stride-to-stride variation in muscle length, activation, force and work per cycle. To investigate mechanisms for stride to stride variation, we used mouse EDL muscles in *ex vivo* work loop experiments as an avatar for *in vivo* guinea fowl LG muscles. Our study used four strain trajectories from a single trial of perturbed running on a treadmill over obstacles at a speed of 2 m s^{-1}. We included strides up onto and down from obstacles attached to the treadmill, as well as unperturbed strides between obstacles. For comparison, we also included a purely sinusoidal strain trajectory at the same amplitude and frequency. This experimental design using *ex vivo* work loops allowed us to investigate how muscle intrinsic properties and stimulation interact to produce the variability in muscle force observed during perturbed *in vivo* locomotion. We also evaluated the ability of traditional sinusoidal work loops at the same frequency to predict muscle force. We used a combination of five strain trajectories and three stimulation patterns to examine the effects of variation in strain, stimulation and their interaction on muscle force and work in *ex vivo* work loops.

Based on Daley and Biewener (2011), we expected that muscle force production during active shortening would be associated not with length or velocity per se, but with abrupt changes in strain rate (i.e. strain transients) similar to those that result *in vivo* from variable loading associated with foot contact in different strides. Therefore, we predicted that *in vivo* strain trajectories from guinea fowl LG imposed on *ex vivo* mouse EDL muscles in avatar work loops would better explain stride-to-stride variations in muscle force than sinusoidal work loops that lack strain transients at the same amplitude and frequency. In purely isometric contractions, muscle force is related to activation, but during unexpected perturbations, muscles respond to changes in load faster than reflexes can modulate activation (Nichols and Houk, 1976). Therefore, we investigated the relative contributions of strain trajectories, stimulation patterns and their interaction on the timing and magnitude of peak muscle force and work per cycle in avatar work loop experiments.

MATERIALS AND METHODS

Muscle preparation

EDL muscles (see fig. 1 of Chleboun et al., 1997) from 60–130 day old male wild-type mice (*Mus musculus*, n=6 muscles, each from a different mouse) of the strain B6C3Fe a/a-Ttn^{mdm}/J were used in this study. Breeder mice were obtained from the Jackson Laboratory (Bar Harbor, ME, USA) and a colony was established at Northern Arizona University (NAU). Mice were fed *ad libitum* and euthanized just prior to muscle extraction. The Institutional Animal Care and Use Committee at NAU approved the use of animals and experimental protocol.

EDL muscles were surgically exposed and 4-0 silk sutures were tied in square knots at the distal and proximal muscle–tendon junctions. Tendons were cut outside the suture knots and muscles were removed for *ex vivo* experiments. Extracted EDL muscles were attached to a dual-mode muscle lever system (Aurora Scientific, Inc., Series 300B, Aurora, ON, Canada) via tightened slip knots in the suture at the ends of the muscle. During experiments, the muscles were bathed in a 21°C, 7.4 pH Krebs–Henseleit solution containing (in mmol l^{-1}): NaCl 118, KCl 4.75, $MgSO_4$ 1.18, $NaHCO_3$ 24.8, KH_2PO_4 1.18, $CaCl_2$ 2.54 and glucose 10.0. The bath was aerated with a 95% O_2/5% CO_2 gas mixture. The muscle was suspended between two platinum electrodes which delivered 1 ms square-wave pulses at tetanic supramaximal stimulation (80 V, 200 Hz) while finding optimal length (L_0). Submaximal stimulation (45 V, 90 Hz) was used during the experimental protocol to more closely emulate *in vivo* activation, and to decrease fatigue during experimental trials (James et al., 1995).

After finding L_0, a series of 80 V conditioning twitches was delivered to the muscle until twitch force reached a steady state (Hakim et al., 2013). Isometric force after a 500 ms tetanus was measured at L_0 using submaximal stimulation before and after the experimental protocol to measure fatigue. Muscles that lost more than 10% force (n=1) were not included in the analysis. After all experimental trials were completed, the muscle was removed from the rig, the sutures were removed, and the muscle was dabbed dry once and weighed. Physiological cross-sectional area (PCSA) was calculated using the standard formula: muscle mass/(L_0×1.06 g cm^{-3}).

Journal of Experimental Biology (2023) 226, jeb244721. doi:10.1242/jeb.244721

Using *in vivo* lateral gastrocnemius parameters in *ex vivo* EDL work loops

In a previous study (Daley and Biewener, 2011), strain trajectories, activation and force were measured *in vivo* from the lateral gastrocnemius (LG) of guinea fowl during running with obstacle perturbations on a treadmill, using sonomicrometry, EMG and tendon buckles (see fig. 1 of Daley and Biewener, 2003). Obstacle perturbations induced high stride-to-stride variability in muscle strain, activation and force (Fig. 1A). The guinea fowl LG muscle produced up to 40 times more work per cycle when the bird stepped up onto the obstacle than when it stepped down from the obstacle (Fig. 1A, compare red and gold lines). Additionally, the delay between EMG onset and force onset varied from as little as 20 ms for steps up onto the obstacle (Fig. 1A, red line) to more than 150 ms for steps down from the obstacle (Fig. 1A, gold line).

In vivo strain trajectories obtained from a single bird (Bl3; see Dryad dataset https://doi.org/10.7280/D11H49) running over obstacles at a speed of 2.0 m s^{-1} (Fig. 1A) were used to control the length of the mouse EDL muscles during *ex vivo* work loop experiments (Fig. 1B). To investigate the function of the guinea fowl LG during different types of strides, we used LG strain trajectories from four strides of a guinea fowl's instrumented leg in *ex vivo* EDL work loop experiments: one stride in which the leg stepped down from the obstacle onto the treadmill (Fig. 1A; 'Down', gold line); two in which the instrumented leg stepped up from the treadmill onto the obstacle (Fig. 1A; 'Up1', purple line, and 'Up2', red line); and one in which no obstacle was present (Fig. 1A, 'No obstacle', blue line). We included two different Up trajectories because Up1 had a small stretch in the strain trajectory, whereas Up2 did not (Fig. 1A). Each of the strain trajectories was used in *ex vivo* EDL work loops at 2 Hz, although the *in vivo* guinea fowl strain trajectories varied in frequency from 2.85 to 3.34 Hz. The frequency was kept constant in the *ex vivo* experiments to isolate the effect of strain trajectory. Because *in vivo* data were sampled at a higher rate (10,000 Hz) than *ex vivo* data (4000 Hz), the *in vivo* data were down-sampled using MATLAB so that EDL strain, stimulation and force (Fig. 1B) were represented by 2000 data points per cycle. For each muscle, we also included passive and active sinusoidal work loops at the same strain amplitude and frequency. Two work loop cycles were performed for each strain trajectory. In preliminary studies (Rice, 2020), we tested mouse EDL muscles at different starting lengths (i.e. −10% L_0, −5% L_0, L_0, L_0+5%) and stretch amplitudes (10–20% L_0). Preliminary experiments using the Up1 strain trajectory suggested that an initial length of L_0−5% and a final length of L_0+5% best emulated the rate of increase in tension observed during passive stretch of the *in vivo* guinea fowl LG from 83.4% to 122.9% L_0 (see Table 1 and Fig. 1A).

Stimulation patterns for the *ex vivo* EDL work loops were based on measured *in vivo* guinea fowl EMG, which typically starts at the longest muscle length at the onset of leg retraction (Daley and Biewener, 2011), but starts ∼30 ms later in some birds (e.g. Ye3 in Dryad dataset https://doi.org/10.7280/D11H49). To measure effects of variation in stimulation patterns on work loop variables, all five strain trajectories were tested using three different stimulation patterns (EMG-based, Late and Long) at the same submaximal stimulation level (45 V, 90 Hz). On average, submaximal stimulation produced 91% of the maximum isometric force observed during supramaximal stimulation. At stimulation levels lower than 45 V and 90 Hz, the force in sinusoidal work loops was unfused. The onset and duration of the EMG-based stimulation pattern (Fig. 2A) used in the *ex vivo* EDL work loops was based on observed EMG data from the guinea fowl LG for the Up1 step. We accounted for the differing delay between activation and force onset, measured at ∼25 ms *in vivo* (Daley and Biewener, 2011) versus only 4–5 ms in *ex vivo* experiments, by stimulating EDL muscles 20 ms later than observed *in vivo*. Thus, EMG-based stimulation began 20 ms after the longest muscle length and continued for a duration of 115 ms as observed *in vivo* during the Up1 step (Daley and Biewener, 2011).

Late stimulation (Fig. 2B) was based on observed variation in EMG onset among birds (Daley and Biewener, 2011) and started

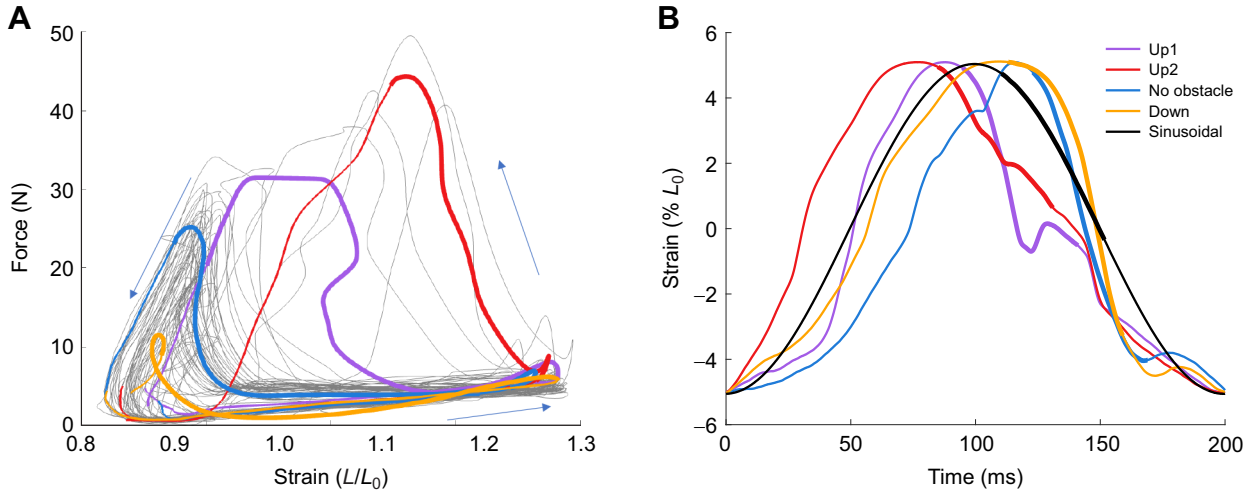

Fig. 1. Methods for using *in vivo* strain trajectories from guinea fowl lateral gastrocnemius (LG) in *ex vivo* work loop experiments on mouse extensor digitorum longus (EDL). (A) Work loops measured *in vivo* from guinea fowl LG (from Daley and Biewener, 2011), where strain is given as length over optimal length (L/L_0). Purple (Up1) and red (Up2) lines show strides up onto an obstacle, gold (Down) shows a stride down from an obstacle, and blue (No obstacle) is a stride with no obstacle present. Thicker lines indicate the timing of muscle activation. Gray lines show guinea fowl strides from the same trial that were not used in the avatar experiments. *In vivo* guinea fowl LG muscles are typically activated at approximately their longest length. (B) *In vivo* strain trajectories from guinea fowl LG shown in A were scaled and used in work loop experiments on *ex vivo* mouse EDL muscles. Colors indicate corresponding strain trajectories. Thicker lines indicate the timing of muscle stimulation. The black line shows a sinusoidal strain trajectory with the same strain amplitude (−5% to +5% L_0), frequency (2 Hz) and stimulation [electromyography (EMG) based, see Fig. 2]. Stride frequencies for the guinea fowl strides were as follows: Up1 2.85 Hz, Up2 2.95 Hz, No obstacle 2.97 Hz, Down 3.34 Hz.

Table 1. Characteristics of guinea fowl lateral gastrocnemius (LG) and mouse extensor digitorum longus (EDL) muscles, and the ratio of their values

Characteristic	Guinea fowl LG	Mouse EDL	Ratio
Muscle geometry	Unipennate	Unipennate	
Pennation angle (deg)	24	12	2:1
Muscle mass (g)	8	$12.8\pm1.6\times10^{-6}$	627,450:1
L_0 fascicle (mm)	17.5*	14.6‡	1.2:1
Length range (mm)	14.6–21.5	13.8–15.3	3.84:1
Strain range (% L_0)	83.4–122.9	97.1–107.4	4.5:1
PCSA (cm^2)	4.1	0.0088±0.0008	461:1
P_0 (N)	129.0§	0.31±0.04	416:1
Maximum isometric stress (N cm^{-2})	31.5*	35.2	0.89:1
Maximum observed force (N)	44.3	0.25±0.03	177:1
Maximum observed stress (N cm^{-2})	10.9	28.1±2.07	0.39:1

Guinea fowl (BL3) LL data are from Dryad (https://doi.org/10.7280/D11H49). For the mouse EDL, values are means±s.d. (n=6). L_0, optimal length; PCSA, physiological cross-sectional area; P_0, peak stress. *Estimated from *in situ* data on other individual birds. ‡Estimated from pennation angle and muscle length. §Estimated as 31.8 N cm^{-2} from *in situ* data on other individual birds.

32.5 ms later than for EMG-based stimulation, for the same duration of 115 ms, occurring at the onset of increased muscle shortening velocity. Long stimulation (Fig. 2C) spanned the other two, as the muscle was stimulated at the same time as EMG-based stimulation, but was deactivated at the same time as Late stimulation, for an average duration of 148.4 ms (range 122 ms for Up1 to 156.25 ms for Down). Because the timing of stimulation onset was controlled relative to muscle length rather than cycle phase, the average duration varied among the strain trajectories. The order in which strain trajectories and stimulation patterns were performed was randomized for each muscle. In total, 15 work loops were performed on each muscle, including all combinations of five strain trajectories and three stimulation patterns.

Statistical analysis

The coefficient of determination (R^2) was used to quantify the proportion of variance of *in vivo* guinea fowl LG force that was explained by the *ex vivo* mouse EDL force using the same strain trajectories. All 2000 data points per cycle were used to calculate R^2 values. The data were highly consistent within and between muscles. Given the observed standard deviations, the sample size of n=6 mice per group was sufficient to detect large effects (20% difference in group means) with power >0.8. The untransformed data for all five dependent variables (work per cycle; peak stress; muscle strain at peak stress; muscle strain at active stress onset; and time from muscle stimulation to peak stress) had non-homogeneous variances (Levene's test, P<0.05), and only peak stress was normally distributed (Shapiro–Wilk test, P<0.05). No transformations that we tried, including Box–Cox, succeeded in normalizing the data or equalizing the variances. Because the size of all model effects (stimulation pattern, strain trajectory and stimulation pattern×strain trajectory) was large for all dependent variables (P<0.008–0.0001), and because we were interested in the relative size of the main effects and their interaction, we conducted a three-way factorial analysis of variance despite violation of assumptions. ANOVA is generally robust for analysis of non-normal data even when sample sizes are small (Blanca et al., 2017), and also robust for analysis of heteroscedastic data when the sample sizes are equal (Glass et al., 1972). We also checked for non-independence of the five dependent variables using principal component analysis. When dependent variables are highly intercorrelated, the first principal component typically explains a high proportion (>75%) of the variance. For the work loop variables considered here, principal components 1–5 explained 39.8%, 25.7%, 17.3%, 14.1% and 3.1% of the total variance, respectively, demonstrating relatively low levels of intercorrelation.

Three-way mixed-model ANOVA was performed using JMP (version 14, SAS Institute Inc., Cary, NC, USA) to determine how stimulation (EMG-based, Late, Long; d.f.=2), strain trajectory (Up1, Up2, Down, No obstacle and Sinusoidal; d.f.=4) and their interaction affected work loop variables (peak stress, work per cycle, muscle strain at peak stress, muscle strain at force onset and

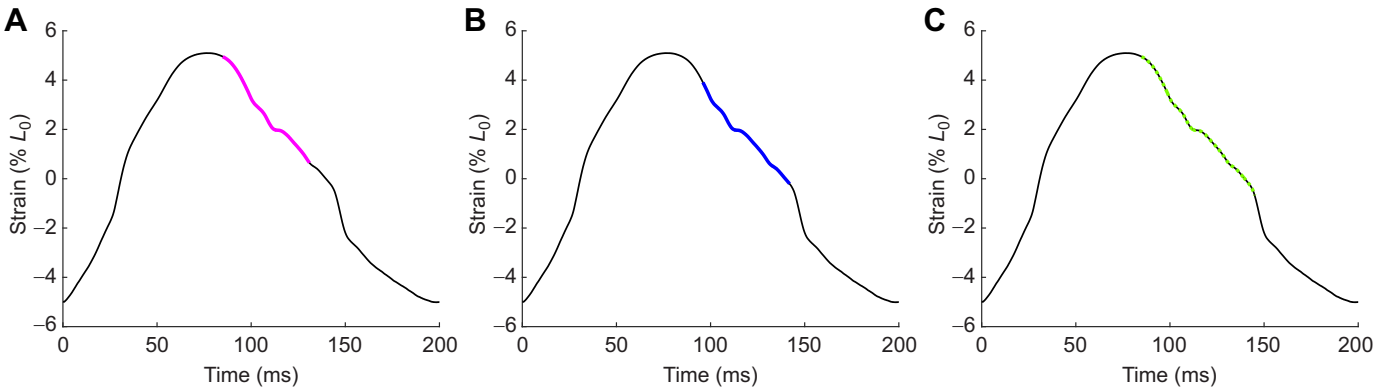

Fig. 2. Timing of stimulation patterns used in mouse EDL work loops as a function of strain. (A) EMG-based (pink), (B) Late (blue) and (C) Long stimulation (dotted green) for a representative strain trajectory (Up2). EMG-based stimulation starts 20 ms after the muscle reaches its longest length, with a duration of 115 ms. Late stimulation begins ∼33 ms later with a duration of 115 ms. Long stimulation begins at the same time as EMG-based and ends at the same time as Late stimulation, with an average duration of 148.4 ms.

Journal of Experimental Biology (2023) 226, jeb244721. doi:10.1242/jeb.244721

time from stimulation onset to peak stress). The main effects were strain trajectory (fixed), stimulation pattern (fixed) and animal (random; d.f.=5). The interactions included animal×strain trajectory (random), animal×stimulation pattern (random), strain trajectory × stimulation (fixed) and animal×strain trajectory×stimulation pattern (random). Random effects, while sometimes significant, were not reported in ANOVA tables because they were not of interest in this study. To measure the relative size of the fixed effects (strain trajectory, stimulation pattern and strain trajectory×stimulation pattern), we analyzed FDR (false discovery rate) logWorth values. Tukey's honestly significant difference (HSD) test was used to evaluate *post hoc* differences among means.

As all ANOVA model effects were highly significant (P<0.008), we used discriminant function analysis to determine the relative importance of variation in strain trajectory and stimulation pattern in determining work loop variables. Linear discriminant analysis (LDA) and quadratic discriminant analysis (QDA) were performed using JMP to determine whether trials could be discriminated based on the strain trajectories or stimulation patterns from which they were generated using the same dependent variables included in the ANOVA. These analyses were used to determine whether strain trajectory or stimulation pattern causes more distinct grouping of the data. A 50:50 test-to-train ratio was used in which the second of two work loops for each combination of strain trajectory and stimulation for each muscle was used to train the model and the first was used to test the model. Each strain trajectory group included a sample size of 18 work loops and each stimulation pattern group included a sample size of 30 work loops, representing trials with five strain trajectories and three stimulation patterns performed on six muscles for a total of 90 test trials for each discriminant analysis.

RESULTS

Comparison of guinea fowl LG and mouse EDL muscles

The mouse EDL and guinea fowl LG are both unipennate muscles (Table 1). Total muscle length was measured for the *ex vivo* mouse EDL muscle, but fascicle length was measured for the *in vivo* guinea fowl LG (Table 1). Because the pennation angle of the mouse EDL is small (12 deg), the difference between muscle length and fascicle length is also small (<3%). It is important to note, however, that the length and strain estimates from sonomicrometry may differ among locations within a given muscle (Higham and Biewener, 2011), and may not correspond to length measurements made using a servo-motor length sensor.

PCSA differed by a factor of 461 (from a mean of 0.0088 cm^2 in mouse EDL to 4.1 cm^2 in Bl3 LG), and the maximum observed forces differed by a factor of 177, from 0.25 N in mouse EDL (80.6% P_0) to 44.3 N (43.6% P_0) in the guinea fowl LG (Table 1). The observed maximum stress was 28.1 N cm^{-2} for a strain amplitude of 10.3% L_0 in the mouse EDL versus 10.9 N cm^{-2} for a strain amplitude of 39.5% median length in the guinea fowl LG.

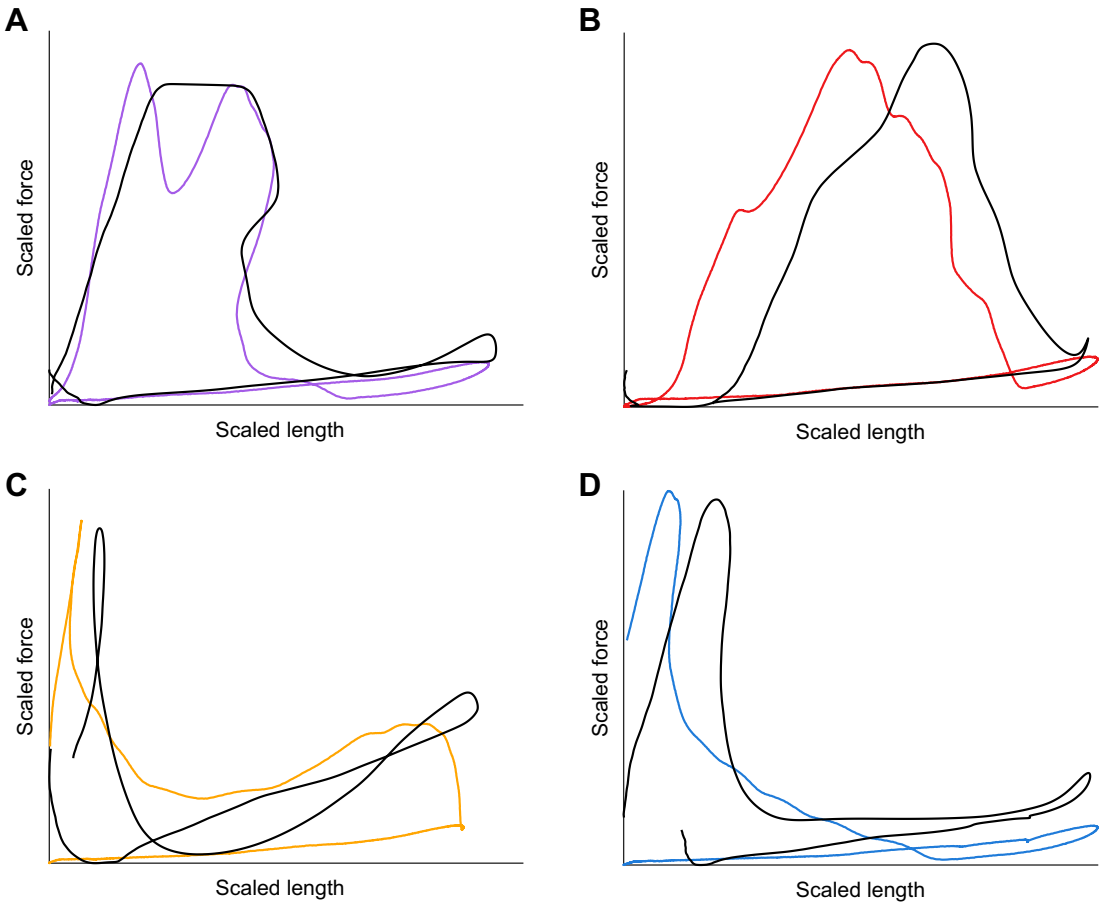

Fig. 3. Given *in vivo* strain trajectories from guinea fowl LG muscles, mouse EDL muscles produce similar work loops. Work loops from *in vivo* guinea fowl LG (black) and a representative *ex vivo* mouse EDL muscle (colors as for Fig. 1) for Up1 with Late stimulation (A, R^2=0.94), Up2 with Late stimulation (B, R^2=0.79), Down with Long stimulation (C, R^2=0.60), and No obstacle with EMG-based stimulation (D, R^2=0.61). R^2 indicates the proportion of variance in guinea fowl LG force explained by EDL force at the same scaled muscle length.

Journal of Experimental Biology (2023) 226, jeb244721. doi:10.1242/jeb.244721

Therefore, the approximate active muscle 'stiffness' was ∼10 times higher for mouse EDL than for guinea fowl LG (Table 1).

Comparison of *in vivo* and *ex vivo* work loops

Ex vivo strain trajectories were approximately sinusoidal (Fig. 1B), although they reached peak strain at different phases and were less symmetrical than the sinusoidal trajectory (Fig. 1B, black line). The average velocity was 0 mm s^{-1} for all strain trajectories. A major difference between the sinusoidal and *in vivo* strain trajectories was that the *in vivo* strain trajectories contained abrupt changes in strain rate (i.e. strain transients) that were absent in the sinusoidal trajectory. During *in vivo* locomotion in the guinea fowl LG, these transients in strain rate correspond to foot contact (Daley and Biewener, 2011). The LG muscles typically reach their maximum shortening velocity immediately before foot contact and their maximum stretch velocity shortly thereafter. For the *ex vivo* experiments, the range of velocity was only 18.1 mm s^{-1} for the sinusoidal trajectory, whereas it varied from 29.7 to 38.2 mm s^{-1} among the *in vivo* strain trajectories.

When *ex vivo* mouse EDL work loops were scaled to the same approximate force and length as *in vivo* guinea fowl work loops (Fig. 3), the shapes of *ex vivo* EDL work loops were similar to the shapes of *in vivo* LG work loops with the same strain trajectory. R^2 values between *in vivo* guinea fowl LG force and *ex vivo* mouse EDL force ranged from 58% to 94%. EDL work loops with different strain trajectories showed distinctive features that were consistent across muscles; so much so, that work loops could be associated with a particular strain trajectory by looking at shape alone. The distinctive features of the work loops are likely due to strain transients that differed among the strain trajectories. The shapes of *ex vivo* mouse EDL work loops were more similar to *in vivo* guinea fowl LG work loops with the same strain trajectory than they were to *ex vivo* EDL work loops with different strain trajectories (Fig. 3).

In general, peak force, work per cycle, muscle strain at peak force and delay between activation/stimulation onset and peak force were similar for guinea fowl LG and mouse EDL, given the same strain trajectory (Fig. 3). The average variance in guinea fowl LG force explained (R^2) by *ex vivo* mouse EDL force was 0.94 for the Up1 strain trajectory with Late stimulation, 0.76 for the Up2 strain trajectory with Late stimulation, 0.58 for the Down strain trajectory with Long stimulation, and 0.69 for the No obstacle strain trajectory with EMG-based stimulation. The variation in R^2 among the different strain trajectories is likely due to the fact that the stimulation patterns, amplitude, starting and ending strain values were optimized only for the Up1 strain trajectory, and those parameters were then applied to the other strain trajectories.

Despite similarities in overall work loop shape, there were differences between mouse EDL and guinea fowl LG (see Table 1). Although similar in length (fascicle L_0=14.6 mm for mouse EDL and 17.5 mm for guinea fowl LG), the mass, PCSA and maximum observed force of the guinea fowl LG were 627, 450, 461 and 177 times greater than those of the mouse EDL, respectively, and as noted previously, the mouse EDL was ∼10 times stiffer. Particularly for the Up1 trajectory, the mouse EDL failed to maintain peak force for as long as was observed in the guinea fowl LG (see Fig. 3A), suggesting that activation/deactivation kinetics are faster in the mouse EDL than in the guinea fowl LG.

In *ex vivo* work loop experiments, mouse EDL muscles exhibited considerable variation in force–length behavior among strain trajectories but with the same stimulation pattern (Fig. 4). The average R^2 was lower across strain trajectories for EDL muscles than within strain trajectories between mouse EDL and guinea fowl LG, keeping stimulation constant. For example, the average R^2 between mouse EDL Up1 Late and the other strain trajectories from the same EDL muscle was 0.29, compared with an R^2 of 0.94 between Up1 Late and the *in vivo* guinea fowl LG force from the same strain trajectory. The average R^2 values for mouse EDL Up1 Late compared with the other strain trajectories from the same muscle were as follows: Up2 Late R^2=0.18, Down Long R^2=0.33, No obstacle EMG-based R^2=0.37. These comparisons suggest that *ex vivo* EDL stress was influenced more by strain trajectory than by muscle type (mouse EDL versus guinea fowl LG) or stimulation pattern (EMG-based, Long or Late).

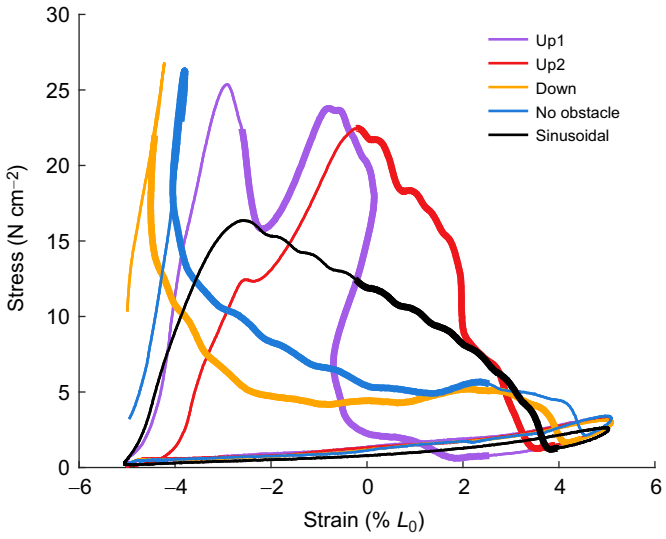

Fig. 4. With the same stimulation, EDL work loops vary among strain trajectories. Work loops from a representative EDL muscle for all five strain trajectories and Late stimulation (see Fig. 2B). Note that the work loop for the sinusoidal trajectory (black) resembles none of the other work loops. Thicker lines indicate the timing of stimulation.

Although the sinusoidal strain trajectory (Fig. 4, black line) looked somewhat similar to Up1 and Up2 strain trajectories and had the same strain amplitude (±5% L_0), frequency (2 Hz) and stimulation patterns, sinusoidal work loops were more rectangular in shape, as observed in previous studies (James et al., 1995, 1996). Regardless of stimulation pattern, sinusoidal strain trajectories lacked the distinguishing shape characteristics of *ex vivo* mouse EDL and *in vivo* guinea fowl LG work loops, and explained only a small proportion of variance in both guinea fowl LG forces for the same strain trajectories (average R^2=0.045, n=4) and mouse EDL forces (average R^2<0.109, n=6), which were nevertheless significantly greater than expected due to chance given the large number of data points (n=2000) on which the calculations were based.

Effect of stimulation patterns on work loops

Although stimulation patterns changed the shape of the EDL work loops, work loops with the same strain trajectory but different stimulation patterns were more similar to each other than work loops with the same stimulation pattern but different strain trajectories (Fig. 5). The effects of stimulation also differed among strain trajectories. All three stimulation patterns produced similar peak stress for the Up2 strain trajectory (Fig. 5B), but for the Down strain trajectory (Fig. 5C), EMG-based stimulation produced lower peak stress compared with the other stimulation patterns.

Journal of Experimental Biology (2023) 226, jeb244721. doi:10.1242/jeb.244721

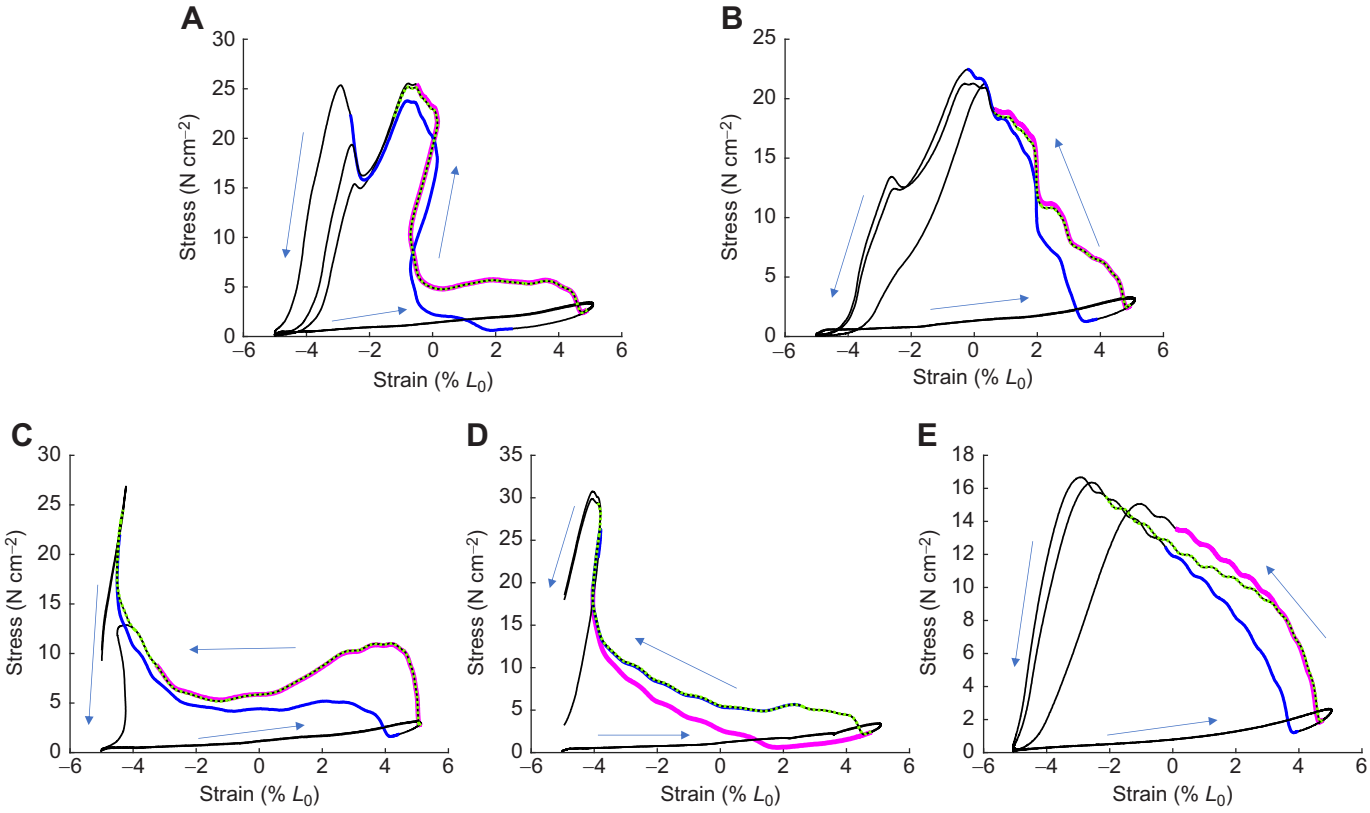

Fig. 5. Effects of stimulation differ among strain trajectories. Work loops for (A) Up1, (B) Up2, (C) Down, (D) No obstacle and (E) Sinusoidal strain trajectories are shown for a representative EDL muscle with EMG-based (pink), Late (blue) and Long (dotted green) stimulation. For the Up2 strain trajectory, the difference between EMG-based and Long stimulation was relatively small, and all three stimulation patterns produced similar peak stress and work per cycle. For the Down strain trajectory, EMG-based and Long stimulation were similar initially, but EMG-based stimulation produced lower peak stress than Late or Long stimulation. Thicker lines indicate the timing of stimulation. The direction of the work loops is counterclockwise as shown by blue arrows.

Effects of strain, stimulation and strain×stimulation on work loop variables

Peak stress

Strain trajectory, stimulation pattern and the strain×stimulation interaction had significant effects on peak stress (ANOVA, all P<0.0001; Table 2). No obstacle (mean±s.d. 25.7±0.60 N cm^{-2}), Up1 (24.6±0.5 N cm^{-2}) and Up2 (22.5±0.74 N cm^{-2}) produced the highest peak stress, Down (21.3±1.2 N cm^{-2}) produced significantly less stress than No obstacle and Up1, but was not statistically different from Up2, and the sinusoidal trajectory (12.8 ± 1.2 N cm^{-2}) produced significantly lower peak stress than all other strain trajectories (Tukey HSD, all P<0.05; Fig. 6C). Late and Long stimulation produced significantly higher peak stress than EMG-based stimulation (Tukey HSD, all P<0.05). The interaction between strain trajectory and stimulation had a larger effect (FDR logWorth=24.4; Table 2) on peak stress than strain trajectory (FDR logWorth=7.7) or stimulation (FDR logWorth=7.2) alone. The main interaction effect was that all stimulation patterns produced nearly the same peak stress for Up1, Up2 and sinusoidal trajectories, but EMG-based stimulation produced significantly lower peak stress for the No obstacle and Down trajectories (Tukey HSD, all P<0.05; Fig. 7A).

Work per cycle

Strain trajectory, stimulation and their interaction had significant effects on work per cycle (ANOVA, all P<0.0001; Table 2). Among strain trajectories, Up2 (115.9±7.1 mJ) and sinusoidal (89.6±10.5 mJ) produced significantly more work than Up1 (86.4±4.9 mJ), Down (86.6±7.3 mJ) and No obstacle (71.2 ±4.7 mJ; Tukey HSD, all P<0.05; Fig. 6A). Among activation patterns, Long stimulation produced significantly more work per

Table 2. ANOVA results for work loop variables

Model effects	d.f.	*F*-ratio	*P*-value	FDR logWorth
Work per cycle				
Strain trajectory	4	52.5144	**<0.0001**	9.426
Stimulation pattern	2	35.9652	**<0.0001**	4.567
Strain×Stimulation	8	54.5168	**<0.0001**	17.897
Length at stress onset				
Strain trajectory	4	5.4938	**0.0038**	2.425
Stimulation pattern	2	51.8386	**<0.0001**	4.801
Strain×Stimulation	8	5.9279	**<0.0001**	4.111
Peak stress				
Strain trajectory	4	33.4767	**<0.0001**	7.699
Stimulation pattern	2	134.1832	**<0.0001**	7.223
Strain×Stimulation	8	122.0134	**<0.0001**	24.422
Length at peak stress				
Strain trajectory	4	36.4263	**<0.0001**	7.715
Stimulation pattern	2	16.8838	**0.0006**	3.030
Strain×Stimulation	8	3.1055	**0.0080**	2.095
Time: activation to peak stress				
Strain trajectory	4	9.8231	**0.0001**	3.837
Stimulation pattern	2	57.4678	**<0.0001**	5.006
Strain×Stimulation	8	5.8836	**<0.0001**	4.080

False discovery rate (FDR) logWorth was used to quantify the relative size of each model effect. Significant values are in bold.

Journal of Experimental Biology (2023) 226, jeb244721. doi:10.1242/jeb.244721

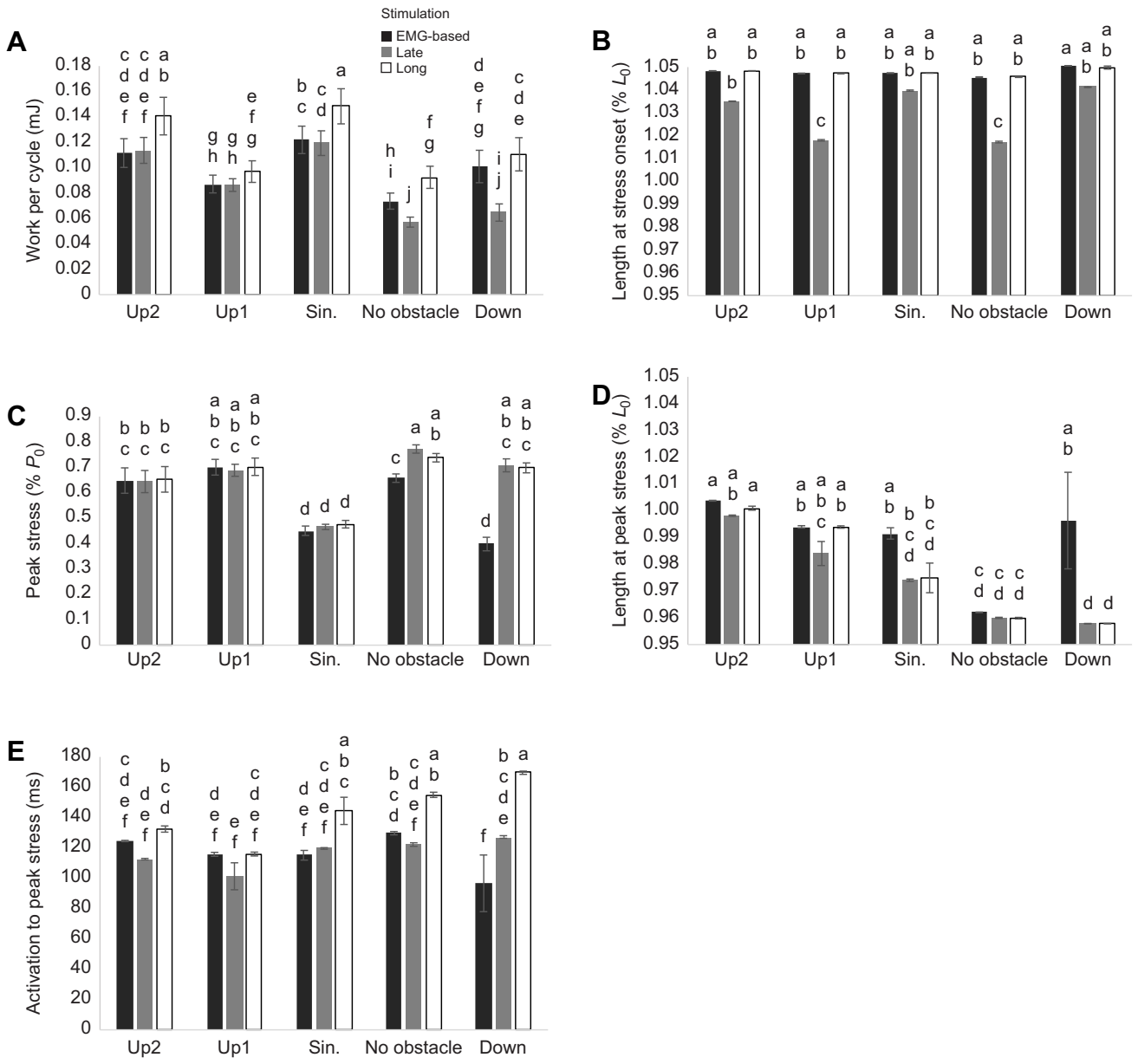

Fig. 6. Work loop variables differ among strain trajectories and stimulation patterns. (A) Work per cycle. (B) Length at stress onset. (C) Peak stress (P_0). (D) Length at peak stress. (E) Time from stimulation onset to peak stress. Means±s.e.m.; bars not connected by the same letter are significantly different (n=6 muscles, ANOVA, Tukey HSD, P<0.05).

cycle than the other stimulation patterns, and Late stimulation produced more work per cycle than EMG-based stimulation (Tukey HSD, all P<0.05). The main interaction effect was that EMG-based and Late stimulation produced nearly the same work per cycle for Up1, Up2 and sinusoidal strain trajectories, but Late stimulation produced more work per cycle than EMG-based stimulation for No obstacle and Down strain trajectories (Tukey HSD, all P<0.05; Fig. 6A). The interaction between strain trajectory and stimulation pattern had a larger effect on work per cycle (FDR logWorth=17.9) than either strain trajectory (9.4) or stimulation (4.6) alone (Table 2).

Muscle strain at peak stress

Strain trajectory, stimulation and the strain trajectory×stimulation interaction had significant effects on muscle strain at peak stress (ANOVA, all P<0.01; Table 2). Muscle strain at peak stress was significantly higher for Up1 (0.99±0.001% L_0) and Up2 (1.00±0.0004% L_0) compared with No obstacle (0.96±0.0002% L_0), Down (0.97±0.005% L_0) and Sine (0.98±0.002% L_0; Tukey HSD, all P<0.05; Fig. 6D). EMG-based stimulation produced significantly larger strains at peak stress than other stimulation patterns (Tukey HSD, all P<0.05). The main interaction effect was that all stimulation patterns produced nearly the same strain at peak stress for Up1, Up2 and No obstacle, but EMG-based stimulation produced significantly larger strains at peak stress for the Sinusoidal and Down trajectories (Tukey HSD, all P<0.05; Fig. 7A). Strain trajectory had a larger effect (FDR logWorth=7.7; Table 2) on strain at peak stress than stimulation (FDR logWorth=3.0), or strain trajectory×stimulation (FDR logWorth=2.1).

Journal of Experimental Biology (2023) 226, jeb244721. doi:10.1242/jeb.244721

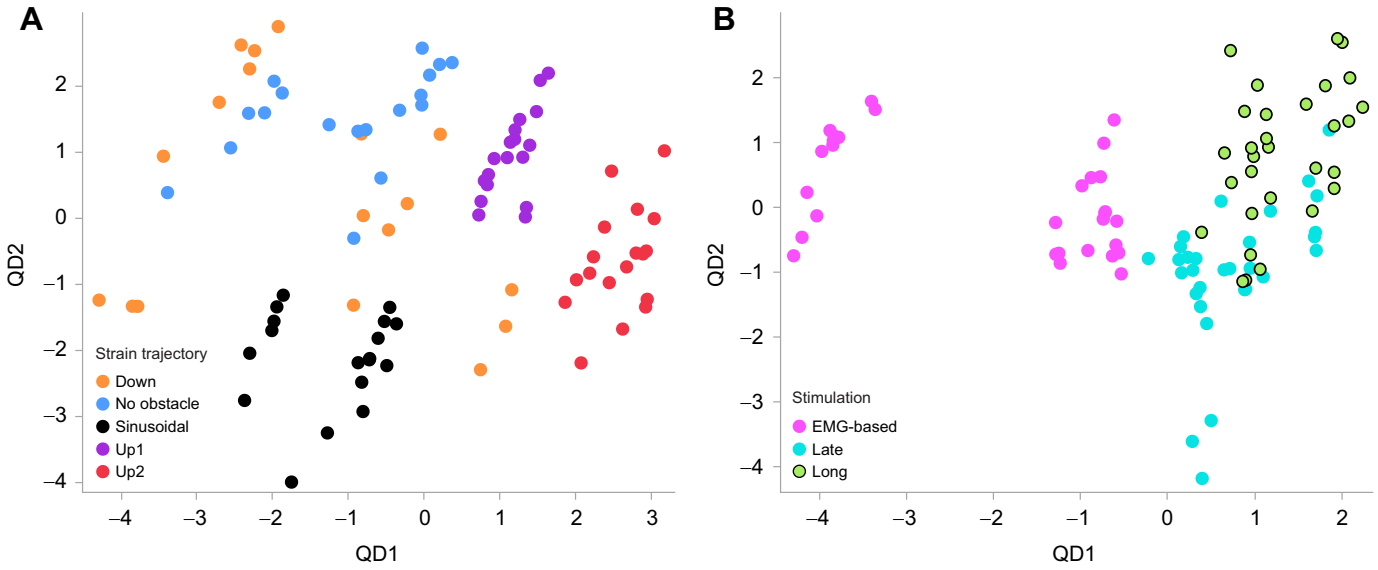

Fig. 7. Discriminant function analysis of work loops. (A) Work loops with the same strain trajectory cluster more closely than (B) work loops with the same stimulation pattern. Results from quadratic discriminant analysis (QDA; n=90). Classification based on strain trajectory was 100% correct whereas classification based on stimulation pattern was 84.4% correct. In A, note that the Down trajectory (gold) was more sensitive to stimulation pattern than the other strain trajectories. See Results for details. QD, quadratic discriminant function.

Muscle strain at stress onset

Strain trajectory, stimulation and their interaction had significant effects on muscle length at active stress onset (ANOVA, all P<0.005; Table 2). Sinusoidal (1.045±0.001% L_0), Up2 (1.044±0.001% L_0) and Down (1.044±0.004% L_0) trajectories developed stress at a significantly longer length than Up1 (1.037±0.002% L_0) and No obstacle (1.036±0.002% L_0; Tukey HSD, all P<0.05; Fig. 6A). Strain at stress onset was significantly lower with Late than with EMG-based or Long stimulation (Tukey HSD, all P<0.05). The main interaction effect was that EMG-based and Long stimulation had nearly the same strain for all trajectories except Down, where EMG-based stimulation produced significantly higher strain at stress onset than Long stimulation. Late stimulation produced significantly lower strain than the other stimulation patterns for Up1, Up2 and No obstacle trajectories, but was not statistically different from Long stimulation for the Down trajectory. All stimulation patterns produced nearly the same strain at stress onset for the Sinusoidal strain trajectory (Tukey HSD, all P<0.05; Fig. 6B). Stimulation had a larger effect (FDR logWorth=4.801; Table 2) on strain at stress onset than strain trajectory×stimulation (FDR logWorth=4.111) or strain trajectory (FDR logWorth=2.425).

Time from stimulation onset to peak stress

Strain trajectory, stimulation and their interaction had significant effects on time from activation onset to peak stress (ANOVA, P=0.001; Table 2). No obstacle (136±2.4 ms), Sine (126±3.1 ms) and Down (131±6.5 ms) produced statistically similar times from stimulation to peak stress. Up1 (111±2.5 ms) produced the shortest time, but was not statistically different from Up2 (123±1.5 ms; Tukey HSD, all P<0.05; Fig. 6E). Long stimulation produced significantly longer times from stimulation to peak stress than other stimulation patterns (Tukey HSD, all P<0.05). The main interaction effect was that all stimulation patterns produced times that were not statistically different for the Up1 and Up2 strain trajectories. Long stimulation produced significantly longer times for No obstacle, Sinusoidal and Down trajectories. EMG-based and Late activation produced nearly the same times for all trajectories except Down, while Late stimulation produced significantly longer times (Tukey HSD, all P<0.05; Fig. 7A). Stimulation had a larger effect (FDR logWorth=5.006; Table 2) on time from stimulation to peak stress compared with strain trajectory×stimulation (FDR logWorth=4.080) and strain trajectory (FDR logWorth=3.837).

In summary, strain at stress onset and time from stimulation to peak stress were more affected by stimulation than by strain trajectory or the interaction between these variables. Strain at peak stress was most affected by strain trajectory, while work per cycle and peak stress were more affected by the strain trajectory×stimulation interaction.

Discriminant analysis

Because strain trajectory, stimulation pattern and their interaction had highly significant effects (P<0.008) on all work loop variables, we used discriminant function analysis to quantify how the strain trajectories (Fig. 7A) and stimulation patterns (Fig. 7B) cluster in the space defined by the five work loop variables included in the ANOVA. QDA was more accurate than LDA in classifying the trials, likely because it allows for unequal covariances among groups. Using the work loop variables to categorize strain trajectories (Fig. 7A), QD1 and QD2 explained 98.2% of the total information (entropy R^2), with length at peak stress and peak stress having the highest weightings. All strain trajectories were classified 100% correctly (n=18 for each strain trajectory).

Results of the QDA analysis to classify stimulation patterns (Fig. 7B) showed that QD1 and QD2 explained 74.5% of total information, with time from stimulation to peak stress and work per cycle having the highest weightings. Five Late stimulation trials were misclassified as Long, while nine Long stimulation trials were misclassified as Late (14 of 90 trials misclassified, 84.4% correct). The results from this dataset show that variation among trials in all work loop variables considered simultaneously was more closely related to strain trajectory than to stimulation pattern.

DISCUSSION

Compared with traditional *ex vivo* methods for investigating muscle mechanics (e.g. isometric force–length and isotonic force–velocity

characteristics; Caiozzo, 2002), the work loop technique (Josephson, 1985) revolutionized the way *ex vivo* muscle function is investigated (Ahn, 2012), by stimulating muscles during sinusoidal oscillations in length at a frequency, phase and duty cycle similar to conditions that muscles experience during steady *in vivo* locomotion (Josephson, 1985, 1999). These studies enabled estimation of the work and power that muscles can produce under *in vivo* conditions, compared with their maximum power output (Askew and Marsh, 1997, 2001), and further showed that saw-tooth trajectories, with more variable strain rates than purely sinusoidal strain trajectories, produce more force, work and power (Marsh, 1999). Like the present study, many previous studies used *ex vivo* work loops with *in vivo* strain and activation; for example, sonomicrometry and EMG recordings from quail pectoralis during vertical take-off (Askew and Marsh, 2001). However, these studies were based on *in vivo* strain trajectories under steady conditions in which cycle-to-cycle variability in muscle strain is relatively small (see fig. 2B of Askew and Marsh, 2001).

The novelty of the avatar method is to use a widely studied and readily available muscle (i.e. mouse EDL) to represent a different muscle in *ex vivo* work loop experiments. The method can be used to investigate muscle mechanics under *in vivo*-like conditions for muscles and species that are otherwise unsuitable for *ex vivo* experimentation, including humans and other large animals. In the present study, we used the avatar method to investigate mechanisms that lead to the large variability in peak muscle force and work exhibited *in vivo* by the guinea fowl LG muscle during perturbed locomotion.

Perturbations provide insights into muscle intrinsic properties that are not evident under steady-state conditions (Daley and Biewener, 2011; Shorter and Rouse, 2018; Sponberg et al., 2023). This study used cyclical length changes in *ex vivo* experiments to understand how muscles function during perturbed *in vivo* locomotion. The results of this study demonstrate that: (1) *ex vivo* mouse EDL work loops explained a large proportion (58–94%) of the variance in the *in vivo* force of guinea fowl LG given similar strain and stimulation, despite many differences between muscles and conditions; (2) strain trajectory, stimulation pattern and strain trajectory×stimulation interaction had highly significant (P<0.008) effects on all work loop variables, and for peak stress and work per cycle the interaction effect was larger than the effects of either strain trajectory or stimulation pattern alone; and (3) *in vivo* strain trajectories produced consistent *ex vivo* work loops that could be identified with high accuracy (100%) based on work loop variables using discriminant function analysis. These results demonstrate that using perturbed strain trajectories derived from *in vivo* measurements significantly improves prediction of stride-to-stride variability in muscle force during *in vivo* perturbed locomotion, compared with sinusoidal strain trajectories that lack strain transients. Strain transients are associated with changes in muscle loading during *in vivo* locomotion (Daley and Biewener, 2011). Because it applies strictly to isotonic contractions, Hill's (1938) force–velocity relationship fails to predict muscle force under conditions of variable strain and load (Libby et al., 2020; Jeong and Nishikawa, 2023). To improve understanding of *in vivo* muscle function under dynamic loading conditions, more investigations that measure strain, activation and force of individual muscles during perturbed locomotion are needed, as well as new *ex vivo* techniques that measure the force response of muscles under varying loading and strain. These efforts should lead to muscle models that can more accurately predict *in vivo* muscle forces.

Ex vivo EDL experiments differed from *in vivo* guinea fowl experiments in several ways. During *in vivo* experiments, there was variation in EMG activity between steps, even between steps of the same type (Daley and Biewener, 2011). In contrast, our experiments used submaximal square-wave electrical stimulation (45 V, 90 Hz). Furthermore, the *ex vivo* and *in vivo* data were from different muscles (LG versus EDL) and animals (guinea fowl versus mouse). Despite these differences, *in vivo* strain trajectories from guinea fowl LG produced highly consistent work loops in mouse EDL with similar variability in peak stress, work per cycle, muscle strain at force onset and delay between stimulation onset and peak force. The average variance in guinea fowl LG force explained by EDL avatar force was 58–94%, with the highest R^2 value obtained for the trial with EMG-based stimulation. The EMG-based stimulation pattern produced significantly lower peak stress for the No obstacle and Down trajectories, which may help to explain why guinea fowl use the *in vivo* activation patterns that they do. No obstacle and Down strides involve more energy dissipation than the other step types, and the EMG-based stimulation pattern generated lower peak stress for these stride types, so that there was less energy to absorb.

The R^2 values from *ex vivo* EDL work loops are similar to or exceed Hill model predictions of *in vivo* muscle forces (Lee et al., 2013; Dick et al., 2017; Wakeling et al., 2021), suggesting that *ex vivo* work loop experiments using muscles from laboratory rodents might serve as an alternative 'model' for understanding *in vivo* muscle mechanics in general. Development of techniques for *ex vivo* muscle stimulation that enable more realistic time-varying amplitudes and frequencies that better emulate *in vivo* activation patterns is an important direction for future studies.

It is somewhat surprising that *ex vivo* work loops from different muscles and animals, with simplified electrical stimulation compared with *in vivo* neural activation, generate forces similar to the *in vivo* LG force when given similar strain trajectories. The overall similarities in force–length behavior between guinea fowl LG and mouse EDL demonstrate the importance of strain, and particularly strain transients, in muscle force production during *in vivo* locomotion. The similarities suggest that the intrinsic viscoelastic properties of muscles play an important role in force production by resisting abrupt changes in length, even with no stretching. The resulting forces are not represented in sinusoidal oscillations or predicted by the isotonic force–velocity relationship (Libby et al., 2020; Nishikawa et al., 2018; Jeong and Nishikawa, 2023).

The present study also included sinusoidal strain trajectories at the same amplitude (±5% L_0) and frequency as the *in vivo* strain trajectories. The sinusoidal strain trajectories produced rectangular-shaped work loops, as described in previous studies (James et al., 1995, 1996), that bore little resemblance (average R^2=0.045) to the triangular and L-shaped work loops produced *in vivo* (see Fig. 3), despite overall similarity to the shapes of the *in vivo* strain trajectories (see Fig. 1B). Sinusoidal strain trajectories also produced significantly lower peak forces than the *in vivo* strain trajectories (see Fig. 6C). The main difference between the sinusoidal and *in vivo* strain trajectories is that the *in vivo* trajectories contain strain transients associated *in vivo* with foot contact that are strongly linked with muscle force onset (see Fig. 1B), whereas the sinusoidal strain trajectory at the same frequency does not.

The results suggest that using sinusoidal, saw-tooth or smoothed *in vivo* strain trajectories in *ex vivo* work loop experiments may result in underestimation of peak forces and may fail to accurately represent *in vivo* muscle mechanics. Many previous studies did not include strain transients in *ex vivo* work loop experiments to

investigate *in vivo* muscle function (Askew and Marsh, 2001; Tytell et al., 2018), in part because they studied swimming and flying where changes in loading are less apparent than in terrestrial locomotion. However, strain transients are likely to occur during non-steady locomotion in any medium, and are expected to have large effects on *in vivo* muscle function.

Studies using the work loop technique have also demonstrated that, by changing the phase of stimulation relative to ongoing length changes, the function of a muscle can change from a motor to a strut, spring or brake (Dickinson et al., 2000; Ahn et al., 2003). These studies revealed the importance of the nervous system in controlling the mechanical output of muscles (Ahn, 2012). However, it is also necessary to consider the stabilizing function of muscle intrinsic properties during unexpected perturbations (i.e. 'preflexes'; Loeb, 1995), which can modulate muscle mechanical output without requiring feedforward or feedback instructions from the nervous system. We found that the strain trajectory has a large influence on peak stress and work per cycle of *ex vivo* muscles. Although the guinea fowl LG is active during shortening and functions mostly like a motor during walking and running (Daley and Biewener, 2011), the *ex vivo* EDL data demonstrate that, given constant activation, strain trajectories strongly influence the peak force and work per cycle that a muscle can produce, increasing positive work during strides up onto an obstacle, and dissipating work during strides down from an obstacle, compared with steady locomotion.

The results of this study support the idea that muscle is an active material whose viscoelastic properties are tuned by activation (Kirsch et al., 1994; Nguyen and Venkadesan, 2020preprint; Nishikawa, 2020). The major difference between this view of muscle and the traditional view of muscle as a motor that produces force in response to activation is that information, not only about activation but also about strain transients, is necessary to predict the force of a tunable material. In *ex vivo* experiments, it is possible to examine the effects of different strain trajectories on force production while holding stimulation constant. Our results demonstrate that the force–length behavior of muscles in work loop experiments is more closely associated with strain trajectory than with stimulation pattern (see Fig. 7). Furthermore, work loop variables including peak force and work per cycle were more affected by the interaction between activation and strain trajectory than by either variable alone (see Fig. 6, Table 2). Only 2 of 5 work loop variables (length at stress onset and time from stimulation to peak force) were more strongly affected by stimulation than by strain trajectory or the interaction between these variables (Fig. 6, Table 2). The *ex vivo* results account for the observed decoupling in time between activation and force during perturbed locomotion of guinea fowl (Daley et al., 2009; Daley and Biewener, 2011), and support the idea that muscle is a tunable viscoelastic material for which activation permits but does not instruct force production. The onset and magnitude of muscle force production are determined not only by activation but also importantly by loads applied to the muscle during interaction with the environment (Nishikawa et al., 2007). Understanding the interaction between strain and activation is key to understanding *in vivo* muscle function.

Limitations

In this study, the muscle mechanics data were highly consistent within and between muscles for all combinations of stimulation patterns and strain trajectories. Future experiments should include validating the avatar method using *in situ* guinea fowl LG muscles. A comparison of results from *ex vivo* mouse EDL muscles with those from *in situ* guinea fowl muscles would enable quantification of the relative contributions of muscle size, fiber type, activation and deactivation kinetics, etc., to muscle force generation. Future experiments should also explore development of techniques for *ex vivo* muscle stimulation that enable more realistic time-varying amplitudes and frequencies that better emulate *in vivo* activation patterns.

Acknowledgements

We thank Benjamin Thiesing for technical assistance. Anthony Hessel, Natalie Holt, Tinna Traustadóttir and Philip Service provided guidance and revisions on earlier versions of this manuscript.

Competing interests

The authors declare no competing or financial interests.

Author contributions

Conceptualization: N.R., C.M.B., M.A.D., K.N.; Methodology: N.R., C.M.B., M.A.D., K.N.; Validation: N.R., C.M.B., K.N.; Resources: K.N.; Data curation: N.R., M.A.D., K.N.; Writing - original draft: N.R., C.M.B., K.N.; Writing - review & editing: N.R., C.M.B., M.A.D., K.N.; Visualization: N.R., C.M.B., K.N.; Supervision: K.N.; Funding acquisition: K.N.

Funding

This research was funded by grants from the National Science Foundation (IOS-2016049 and DBI-2021832) to M.D. and K.N.

Data availability

Data are available from the Dryad digital repository (Nishikawa et al., 2022): https://doi.org/10.5061/dryad.0gb5mkm44.

References

Ahn, A. N. (2012). How muscles function – the work loop technique. *J. Exp. Biol.* **215**, 1051-1052. doi:10.1242/jeb.062752

Ahn, A. N., Monti, R. J. and Biewener, A. A. (2003). *In vivo* and *in vitro* heterogeneity of segment length changes in the semimembranosus muscle of the toad. *J. Physiol.* **549**, 877-888. doi:10.1113/jphysiol.2002.038018

Askew, G. N. and Marsh, R. L. (1997). The effects of length trajectory on the mechanical power output of mouse skeletal muscles. *J. Exp. Biol.* **200**, 3119-3131. doi:10.1242/jeb.200.24.3119

Askew, G. N. and Marsh, R. L. (1998). Optimal shortening velocity (V/V_{max}) of skeletal muscle during cyclical contractions: length-force effects and velocity-dependent activation and deactivation. *J. Exp. Biol.* **201**, 1527-1540. doi:10.1242/jeb.201.10.1527

Askew, G. N. and Marsh, R. L. (2001). The mechanical power output of the pectoralis muscle of blue-breasted quail (*Coturnix chinensis*): the in vivo length cycle and its implications for muscle performance. *J. Exp. Biol.* **204**, 3587-3600. doi:10.1242/jeb.204.21.3587

Askew, G. N., Young, I. S. and Altringham, J. D. (1997). Fatigue of mouse soleus muscle, using the work loop technique. *J. Exp. Biol.* **200**, 2907-2912. doi:10.1242/jeb.200.22.2907

Biewener, A. A., Corning, W. R. and Tobalske, B. W. (1998). In vivo pectoralis muscle force-length behavior during level flight in pigeons (*Columba livia*). *J. Exp. Biol.* **201**, 3293-3307. doi:10.1242/jeb.201.24.3293

Blanca, M. J., Alarcón, R., Arnau, J., Bono, R. and Bendayan, R. (2017). Non-normal data: is ANOVA still a valid option? *Psicothema* **29**, 552-557. doi:10.7334/psicothema2016.383

Caiozzo, V. J. (2002). Plasticity of skeletal muscle phenotype: mechanical consequences. *Muscle Nerve* **26**, 740-768. doi:10.1002/mus.10271

Chleboun, G. S., Patel, T. J. and Lieber, R. L. (1997). Skeletal muscle architecture and fiber-type distribution with the multiple bellies of of the mouse extensor digitorum longus muscle. *Acta Anat.* **159**, 147-155. doi:10.1159/000147977

Clemente, C. J. and Richards, C. (2012). Determining the influence of muscle operating length on muscle performance during frog swimming using a bio-robotic model. *Bioinspir. Biomim.* **7**, 036018. doi:10.1088/1748-3182/7/3/036018

Daley, M. A. and Biewener, A. A. (2003). Muscle force-length dynamics during level versus incline locomotion: a comparison of in vivo performance of two guinea fowl ankle extensors. *J. Exp. Biol.* **206**, 2941-2958. doi:10.1242/jeb.00503

Daley, M. A. and Biewener, A. A. (2011). Leg muscles that mediate stability: mechanics and control of two distal extensor muscles during obstacle negotiation in the guinea fowl. *Philos. Trans. R. Soc. B Biol. Sci.* **366**, 1580-1591. doi:10.1098/rstb.2010.0338

Daley, M. A., Voloshina, A. and Biewner, A. A. (2009). The role of intrinsic muscle mechanics in the neuromuscular control of stable running in the guinea fowl. *J. Physiol.* **587**, 2693-2707. doi:10.1113/jphysiol.2009.171017

Dick, T. J. M., Biewener, A. A. and Wakeling, J. M. (2017). Comparison of human gastrocnemius forces predicted by Hill-type muscle models and estimated from ultrasound images. *J. Exp.Biol.* **220**, 1643-1653. doi:10.1242/jeb.154807
Dickinson, M. H., Farley, C. T., Full, R. J., Koehl, M. A. R., Kram, R. and Lehman, S. (2000). How animals move: an integrative view. *Science* **288**, 100-106. doi:10.1126/science.288.5463.100
Eng, C. M., Konow, N., Tijs, C., Holt, N. C. and Biewener, A. A. (2019). In vivo force-length and activation dynamics of two distal rat hindlimb muscles in relation to gait and grade. *J. Exp. Biol.* **222**, jeb205559. doi:10.1242/jeb.205559
Full, R. J., Stokes, D. R., Ahn, A. N. and Josephson, R. K. (1998). Energy absorption during running by leg muscles in a cockroach. *J. Exp. Biol.* **201**, 997-1012. doi:10.1242/jeb.201.7.997
Glass, G. V., Peckham, P. D. and Sanders, J. R. (1972). Consequences of failure to meet assumptions underlying fixed effects analyses of variance and covariance. *Rev. Ed. Res.* **42**, 237-288. doi:10.3102/00346543042003237
Gordon, A. M., Huxley, A. F. and Julian, F. J. (1966). The variation in isometric tension with sarcomere length in vertebrate muscle fibres. *J. Physiol.* **184**, 170-192. doi:10.1113/jphysiol.1966.sp007909
Gordon, J. C., Holt, N. C., Biewener, A. and Daley, M. A. (2020). Data from: tuning of feedforward control enables stable muscle force-length dynamics after loss of autogenic proprioceptive feedback. *eLife* **9**, e53908. doi:10.7554/eLife.53908.sa2
Hakim, C. H., Wasala, N. B. and Duan, D. (2013). Evaluation of muscle function of the extensor digitorum longus muscle ex vivo and tibialis anterior muscle in situ in mice. *J. Vis. Exp.* **72**, 50183. doi:10.3791/50183-v
Hessel, A. L. and Nishikawa, K. C. (2017). Effects of a titin mutation on negative work during stretch–shortening cycles in skeletal muscles. *J. Exp. Biol.* **220**, 4177-4185. doi:10.1242/jeb.163204
Higham, T. E. and Biewener, A. A. (2011). Functional and architectural complexity within and between muscles: regional variation and intermuscular force transmission. *Philos. Trans. R. Soc. Lond. B Biol.* **366**:1477-1487. doi:10.1098/rstb.2010.0359
Hill, A. V. (1938). The heat of shortening and the dynamic constants of muscle. *Proc. Roy. Soc. Lond. B Biol.* **126**, 136-195. doi:10.1098/rspb.1938.0050
Huxley, A. F. (1957). Muscle structure and theories of contraction. *Prog. Biophys. Biophys. Chem.* **7**, 255-318. doi:10.1016/S0096-4174(18)30128-8
Huxley, A. F. (1973). A note suggesting that the cross-bridge attachment during muscle contraction may take place in two stages. *Proc. R. Soc. Lond. B Biol. Sci.* **27**, 83-86. doi:10.1098/rspb.1973.0006
Huxley, H. and Hanson, J. (1954). Changes in the cross-striations of muscle during contraction and stretch and their structural interpretation. *Nature* **173**, 973-976. doi:10.1038/173973a0
Huxley, A. F. and Niedergerke, R. (1954). Structural changes in muscle during contraction: interference microscopy of living muscle fibres. *Nature* **173**, 971-973. doi:10.1038/173971a0
James, R. S., Altringham, J. D. and Goldspink, D. F. (1995). The mechanical properties of fast and slow skeletal muscles of the mouse in relation to their locomotory function. *J. Exp. Biol.* **198**, 491-502. doi:10.1242/jeb.198.2.491
James, R. S., Young, I. S., Cox, V. M., Goldspink, D. F. and Altringham, J. D. (1996). Isometric and isotonic muscle properties as determinants of work loop power output. *Pflügers Archiv.* **432**, 767-774. doi:10.1007/s004240050197
Jeong, S. and Nishikawa, K. (2023). The force response of muscles to activation and length perturbations depends on length history. *J. Exp. Biol.* **226**, jeb.243991. doi:10.1242/jeb.243991
Josephson, R. K. (1985). Mechanical power output from striated muscle during cyclic contraction. *J. Exp. Biol.* **114**, 493-512. doi:10.1242/jeb.114.1.493
Josephson, R. K. (1999). Dissecting muscle power output. *J. Exp. Biol.* **202**, 3369-3375. doi:10.1242/jeb.202.23.3369
Kirsch, R. F., Boskov, D. and Rymer, W. Z. (1994). Muscle stiffness during transient and continuous movements of cat muscle: perturbation characteristics and physiological relevance. *IEEE Trans. Biomed. Eng.* **41**, 758-770. doi:10.1109/10.310091
Lee, S. S. M., Arnold, A. S., de Boef Miara, M., Biewener, A. A. and Wakeling, J. M. (2013). Accuracy of gastrocnemius muscles forces in walking and running goats predicted by one-element and two-element Hill-type models. *J. Biomech.* **46**, 2288-2295. doi:10.1016/j.jbiomech.2013.06.001
Libby, T., Chukwueke, C. and Sponberg, S. (2020). History-dependent perturbation response in limb muscle. *J. Exp. Biol.* **223**, 509646. doi:10.1101/509646
Loeb, G. E. (1995). Control implications of musculoskeletal mechanics. Proceedings of 17th International Conference of the Engineering in Medicine and Biology Society, Montreal, QC, Canada, 2, 393-1394. doi:10.1109/IEMBS.1995.579743
Marsh, R. L. (1999). How muscles deal with real-world loads: the influence of length trajectory on muscle performance. *J. Exp. Biol.* **202**, 3377-3385. doi:10.1242/jeb.202.23.3377
Nguyen, K. D. and Venkadesan, M. (2020). Rheology of tunable materials. *arXiv* arXiv:2005.07238.
Nichols, T. R. and Houk, J. C. (1976). Improvement in linearity and regulation of stiffness that results from actions of stretch reflex. *J. Neurophysiol.* **39**, 119-142. doi:10.1152/jn.1976.39.1.119
Nishikawa, K. (2020). Titin: a tunable spring in active muscle. *Physiology* **35**, 209-217. doi:10.1152/physiol.00036.2019
Nishikawa, K., Biewener, A. A., Aerts, P., Ahn, A. N., Chiel, H. J., Daley, M. A., Daniel, T. L., Full, R. J., Hale, M. E., Hedrick, T. L. et al. (2007). Neuromechanics: an integrative approach for understanding motor control. *Integr. Comp. Biol.* **47**, 16-54. doi:10.1093/icb/icm024
Nishikawa, K. C., Monroy, J. A. and Tahir, U. (2018). Muscle function from organisms to molecules. *Integr. Comp. Biol.* **58**, 194-206. doi:10.1093/icb/icy023
Nishikawa, K., Daley, M., Rice, N. and Bemis, C. (2022). Understanding muscle function during perturbed in vivo locomotion using a muscle avatar approach. Dryad, Dataset. doi:10.5061/dryad.0gb5mkm44
Olberding, J. P., Deban, S. M., Rosario, M. V. and Azizi, E. (2019). Modeling the determinants of mechanical advantage during jumping: Consequences for spring- and muscle-driven movement. *Integr. Comp. Biol.* **59**, 1515-1524. doi:10.1093/icb/icz139
Perreault, E. J., Heckman, C. J. and Sandercock, T. G. (2003). Hill muscle model errors during movement are greatest within the physiologically relevant range of motor unit firing rates. *J. Biomech.* **36**, 211-218. doi:10.1016/S0021-9290(02)00332-9
Rayment, I., Holden, H. M., Whittaker, M., Yohn, C. B., Lorenz, M., Holmes, K. C. and Milligan, R. A. (1993). Structure of the actin-myosin complex and its implications for muscle contraction. *Science* **261**, 58-65. doi:10.1126/science.8316858
Rice, N. (2020). Understanding muscle function during in vivo locomotion using a novel muscle avatar approach. MSc thesis, Northern Arizona University.
Richards, C. T. (2011). Building a robotic link between muscle dynamics and hydrodynamics. *J. Exp. Biol.* **214**, 2381-2389. doi:10.1242/jeb.056671
Richards, C. T. and Clemente, C. J. (2012). A bio-robotic platform for integrating internal and external mechanics during muscle-powered swimming. *Bioinspir. Biomim.* **7**, 016010. doi:10.1088/1748-3182/7/1/016010
Roberts, T. J., Marsh, R. L., Weyand, P. G. and Taylor, C. R. (1997). Muscular force in running turkeys: the economy of minimizing work. *Science* **275**, 1113-1115. doi:10.1126/science.275.5303.1113
Robertson, B. D. and Sawicki, G. S. (2015). Unconstrained muscle-tendon workloops indicate resonance tuning as a mechanism for elastic limb behavior during terrestrial locomotion. *Proc. Natl. Acad. Sci. USA* **112**, E5891-E5898. doi:10.1073/pnas.1500702112
Robertson, B. D., Vadakkeveedu, S. and Sawicki, G. S. (2017). A benchtop biorobotic platform for in vitro observation of muscle-tendon dynamics with parallel mechanical assistance from an elastic exoskeleton. *J. Biomech.* **57**, 8-17. doi:10.1016/j.jbiomech.2017.03.009
Seth, A., Sherman, M., Reinbolt, J. A. and Delp, S. L. (2011). OpenSim: a musculoskeletal modeling and simulation framework for in silico investigations and exchange. *Procedia Iutam.* **2**, 212-232. doi:10.1016/j.piutam.2011.04.021
Shorter, A. L. and Rouse, E. J. (2018). Mechanical impedance of the ankle during the terminal stance phase of walking. *IEEE Trans. Neural Syst. Rehabil. Eng.* **26**, 135-143. doi:10.1109/TNSRE.2017.2758325
Sponberg, S. and Daniel, T. L. (2012). Abdicating power for control: a precision timing strategy to modulate function of flight power muscles. *Proc. R. Soc. B Biol. Sci.* **279**, 3958-3966. doi:10.1098/rspb.2012.1085
Sponberg, S. and Full, R. J. (2008). Neuromechanical response of musculoskeletal structures in cockroaches during rapid running on rough terrain. *J. Exp. Biol.* **211**, 433-446. doi:10.1242/jeb.012385
Sponberg, S., Spence, A. J., Mullens, C. H. and Full, R. J. (2011). A single muscle's multifunctional control potential of body dynamics for postural control and running. *Philos. Trans. R. Soc. Lond. B Biol. Sci.* **366**, 1592-1605. doi:10.1098/rstb.2010.0367
Sponberg, S., Abbott, E. and Sawicki, G. S. (2023). Perturbing the muscle work loop paradigm to unravel the neuromechanics of unsteady locomotion. *J. Exp. Biol.* **226**, jeb243561. doi:10.1242/jeb.243561
Stevens, E. D. (1993). Relation between work and power calculated from force-velocity curves to that done during oscillatory work. *J. Muscle Res. Cell Motil.* **14**, 518-526. doi:10.1007/BF00297214
Sylvester, A. D., Lautzenheiser, S. G. and Kramer, P. A. (2021). A review of musculoskeletal modelling of human locomotion. *Interface Focus* **11**, 20200060. doi:10.1098/rsfs.2020.0060
Tytell, E. D., Carr, J. A., Danos, N., Wagenbach, C., Sullivan, C. M., Kiemel, T., Cowan, N. J. and Ankarali, M. M. (2018). Body stiffness and damping depend sensitively on the timing of muscle activation in lampreys. *Integr. Comp. Biol.* **58**, 860-873. doi:10.1093/icb/icy042
Umberger, B. R. and Rubenson, J. (2011). Understanding muscle energetics in locomotion: new modeling and experimental approaches. *Exerc. Sport Sci. Rev.* **39**, 59-67. doi:10.1097/JES.0b013e31820d7bc5
Wakeling, J. M., Tijs, C., Konow, N. and Biewener, A. A. (2021). Modeling muscle function using experimentally determined subject-specific muscle properties. *J. Biomech.* **117**, 110242. doi:10.1016/j.jbiomech.2021.110242
Zajac, F. E. (1989). Muscle and tendon: properties, models, scaling, and application to biomechanics and motor control. *Crit. Rev. Biomed. Eng.* **17**, 359-411.